Science of the Total Environment 877 (2023) 162925

Contents lists available at ScienceDirect

Science of the Total Environment

journal homepage: www.elsevier.com/locate/scitotenv

Characterization and reuse of waste from the magnesium nitrate fertilizer industry

Sergio Collado, Paula Oulego, Silvia Vázquez, Lucía Pola, Mario Díaz *

Department of Chemical and Environmental Engineering, University of Oviedo, c/ Julián Clavería s/n, E-33071 Oviedo, Spain

HIGHLIGHTS

- A characterization of residues from the liquid fertilizer industry has been made.
- Reintroduction into the manufacturing process is proposed as the best option.
- 86 % on the remaining nitromagnesite in the residue can be recovered by rewashing.
- Rewashing also reduced the initial dry mass of the residue by 77 %.
- Residue should be mixed with quicklime (30 %) to improve its mechanical properties.

GRAPHICAL ABSTRACT

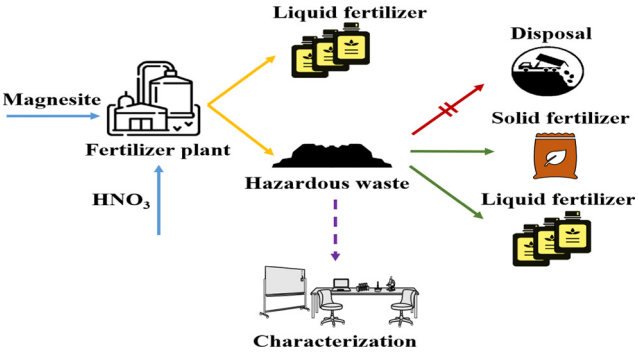

ARTICLE INFO

Editor: Frederic Coulon

Keywords:
Circular economy
Liquid fertilizer
Magnesium nitrate
Nitromagnesite
Valorization

ABSTRACT

Currently, liquid fertilizers are considered strategic products in the sector, particularly those with nitrogen and magnesium in their composition. During their synthesis, the generated muddy and sticky residue is usually managed as a toxic waste because its properties and feasible valorization methods have not yet been studied. For the first time, this residue has been thoroughly characterized, and, on the results obtained, its possible reuse options have been discussed. This material, with 47 % moisture content, a neutral pH, and a specific density of 0.85, still contains 35 % dry weight of nitromagnesite. These findings, together with a high cation exchange capacity and the presence of iron, aluminium, calcium and silicon as minority components, make its reintroduction into the manufacturing process of fertilizers the most viable option for its valorization, having two alternatives for this purpose. The first is to use it as a feedstock for the production of solid fertilizers by adding 30 % quicklime to the residue to improve its mechanical properties, thus obtaining a fertilizer with 5.7 %, 5.0 % and 24.3 % (dry weight) of magnesium, nitrogen and calcium, respectively. The second option, which focused on obtaining a liquid fertilizer, allowed the recovery of approximately 86 % of the remaining nitromagnesite in the residue by washing it with nitric acid, reducing its initial dry mass by 77 %. Then, the resultant liquid phase, with 16 % magnesium nitrate, could be enriched to the 35 % concentration demanded by liquid fertilizer consumers by a subsequent acid attack of the raw rock.

1. Introduction

The growth of the population has caused a steady increase in food consumption, which has led to an expansion of agricultural production (Matamoros et al., 2022). As a result, the worldwide production of fertilizers has maintained an average annual growth rate of 1.7 % over the last decade (Singh et al., 2019) and the Food and Agriculture Organization of

* Corresponding author at: Department of Chemical and Environmental Engineering, University of Oviedo, c/ Julián Clavería s/n, E-33071 Oviedo, Spain.
E-mail address: mariodiaz@uniovi.es (M. Díaz).

http://dx.doi.org/10.1016/j.scitotenv.2023.162925
Received 12 December 2022; Received in revised form 13 March 2023; Accepted 13 March 2023
Available online 17 March 2023

the United Nations (FAO) forecasted that the global demand for nitrogen, phosphorus and potassium for fertilizer use would amount to almost 201,000 thousand tonnes in 2022 (FAO, 2019). For this reason, research has focused on studying the mitigation of the environmental impacts related to their use in agricultural activities (Chojnacka et al., 2019). However, more needs to be done because, despite the increasing attention given to the use of organic wastes as raw materials (Smol, 2021), around 10 million tonnes of inorganic fertilizers are still used only in Europe each year (Eurostat, 2022). In this sense, liquid fertilizers are gaining relevance because they are eco-friendlier and more effective than the traditional solid ones (Intelligence, 2019). Among other advantages, they can be effortlessly distributed by sprinkler or drip irrigation, and easily transported to the roots of plants (Li et al., 2022; Xie et al., 2018).

Regarding fertilizer composition, nitrogen and magnesium are nutrients that are essential for plants and highly improve the growth of the crops (Yousaf et al., 2021). However, magnesium deficiency is becoming more and more prevalent in crops and human intake (Guo et al., 2016; Wang et al., 2020) and nitrogen application causes negative environmental impacts (the presence of nitrates in watercourses or the release of N-containing greenhouse gases, among others) (Gugava and Korokhashvili, 2018; Yousaf et al., 2021). For this reason, fertirrigation is seen as a highly attractive option to solve these problems (García-Saldaña et al., 2019). For example, it was demonstrated that the regular application of specific amounts of liquid N-fertilizers during sprinkler or drip irrigation could reduce the pollution and improve N-use efficiency (Wang et al., 2021).

Therefore, focusing on the production of liquid fertilizers containing N and Mg, the most frequent method used is the acid attack of rocks (Alemrajabi et al., 2019; Matta et al., 2017). On an industrial scale, the common process consists in attacking magnesite ore, previously calcined to improve its reactivity, with nitric acid to obtain a solution rich in magnesium nitrate (Abdel-Aal and Rashad, 1997; Baltrusaitis and Sviklas, 2016). Nevertheless, the solubilization of this mineral is not complete, and the subsequent separation to obtain the liquid phase, or liquid fertilizer, leaves a "muddy residue" formed by the non-solubilized impurities (Baltrusaitis and Sviklas, 2016), which involves considerable disposal costs because its impregnation with a highly concentrated magnesium nitrate solution (and also unreacted nitric acid if the initial dosage was inaccurate) makes it toxic. Furthermore, its wetness and stickiness difficult its handling.

In this context, similar wastes have already been incorporated into other processes. For example, the insoluble by-product of phosphoric acid production (phosphogypsum), obtained during the acid attack of phosphate rock by sulphuric acid, has great potential as an alternative raw material. It can be used as a physical conditioner or chemical amendment for soils, as a substitute for gypsum or even as a source of rare earth elements, among many other applications (Saadaoui et al., 2017; Wu et al., 2018). On the other hand, the calcium nitrate formed when phosphoric rock is attacked with nitric acid can be a raw material for the synthesis of fertilizers. Other examples are the management of the calcium chloride generated during the attack of phosphoric rock with chloride acid, combining rare earth elements recovery with the production of feed-grade calcium hydrogen phosphate, or the retrieval of high-quality gypsum and rare earth elements from the wastes generated during the decomposition of phosphoric rock with phosphoric acid (Wu et al., 2018).

Nevertheless, there was no evidence of an effective circular economy strategy focused on the waste derived from the acid attack of magnesite with nitric acid, but neither its detailed characterization has been carried out. Although extensive research has been done in the past to improve the production process of magnesium nitrate-based fertilizers (for example, see the patents of Gee and Pawel (1951) and William and Neville (1983)), the final sludge is still inevitably generated and, to the best of our knowledge, there is still no research on its valorization. This linear production model is clearly unfeasible as it does not follow the principles of the circular economy (Velenturf and Purnell, 2021) and an in-depth analysis of the properties of this waste is the first necessary step before proposing potential ways of harnessing.

For these reasons, the main aim of this article is to provide, for the first time ever, a complete characterization of the muddy residue obtained from magnesium nitrate production by the fertilizer industry and then, based on the results obtained, to propose and study different methods for its industrial reuse.

2. Materials and methods

2.1. Source material

Samples were taken from the muddy residue generated during magnesium nitrate production by a fertilizer plant (Fertiberia) in Asturias, in Northern Spain. This residue was collected by qualified plant personnel during the production of different batches of this fertilizer for several months in order to ensure its representativeness. It was found that there was practically no variability between those batches. This residue is produced as a result of the attack of the calcined magnesite mineral with nitric acid (57 %). The filtration of the reaction medium results in a liquid phase, the fertilizer, and a clay residue formed by the non-solubilized impurities of the magnesite.

Once collected, the residue, and the subject of this study, was dried at a constant temperature of 105 °C until reaching a constant weight, then crushed in an agate mortar and sieved through a 500 μm sieve to obtain a fine, dry particulate material.

2.2. Characterization

Measurements of moisture, ashes, pH and density were carried out as follows. Moisture was determined by the difference in weight between the raw samples before and after drying in a laboratory oven at 105 °C to constant weight. Subsequently, the dry sample was placed in a muffle furnace at 505 °C for 4 h for the measurement of the ashes by remaining weight (Lipps et al., 2023). The pH was determined in a 1/2.5 (*w*/w) dry clay/water suspension according to the procedure proposed by Saejiew et al. (2004). Finally, densities of either raw (wet) or dry material were calculated by water displacement according to the standard methods (Lipps et al., 2023). All tests were performed in triplicate, so the results shown in the Figures are mean values.

The chemical composition of the muddy residue was analysed using a Shimadzu EDX-720 energy dispersive X-ray fluorescence (XRF) spectrometer. The content of C, H, N and S was determined by elemental analysis with an Elementar Vario EL analyser.

In order to determine the X-ray diffraction patterns (XRD), a powder diffractometer, PANalyticalX'Pert Pro with Cu Kα radiation (λKα = 1.5406 Å) and a secondary graphite monochromator were used. These data were recorded for 2θ values from 10° to 80° using a step of 0.02°, with a scan step time of 1 s. Fourier transform infrared spectroscopy (FTIR) with attenuated total reflectance (ATR) measurements were carried out using a Varian 670 IR spectrometer. The operating conditions of the equipment were 16 scans and a resolution of 4 cm^{-1}. All spectra were taken between 4000 and 400 cm^{-1}.

Cation exchange capacity (CEC) was determined following the barium chloride-triethanolamine method (Alshameri et al., 2018).

A Micromeritics ASAP 2020 instrument was used to perform nitrogen adsorption-desorption tests at 77 K, in order to determine the specific surface area and porous structure of the material. Before such tests, it was necessary to degas the samples at 120 °C for 12 h. Mesoporosity was analysed by the BJH method (Oulego et al., 2020).

The microstructure of the clays and energy-dispersive X-ray analysis were determined by means of a JEOL JMS-6610LV microscope at an acceleration voltage of 20 kV. Before the SEM analysis, the samples were vacuum coated with a thin layer of gold.

In order to determine the microstructure in depth, transmission electron microscopy (TEM) analysis was carried out at 160 kV on a MET JEOL-2000 EX-II microscope. Scanning TEM (STEM) analyses (bright field mode) were performed on a MET JEOL-JEM 2100F microscope operating at 200 kV.

Before analysis, the samples were dispersed in ethanol, sonicated for 1 min and dropped onto carbonated copper grids.

Firmness and stickiness were determined using a TA.XTPlus texture analyser equipped with a 5 kg static load cell and using a single compression cycle test (see Fig. S1 in the Supplementary Material). The operating conditions were a penetration speed of 0.1 mm/s and a penetration depth of 5 mm, using a spherical probe S 0.25. Firmness was defined as the force necessary to reach the maximum depth, and adhesiveness was calculated as the negative force area of the cycle, representing the work necessary to pull the compressing plunger away from the sample (Pressi et al., 2022). Both parameters were calculated employing Exponent software.

2.3. Solubility test

One gram of material, previously dried and sieved through a 500 μm sieve, was added to 200 mL of solvent (water or 57 % nitric acid) and stirred for 24 h at 300 rpm. Afterwards, the final suspension was filtered using an Albet filter with a 12.5 cm diameter in a vacuum flask. The solid obtained was dried in an oven at 105 °C for 24 h, weighed and characterized. Solubility was defined according to the following equation (Eq. 1):

$$(\%)\ \text{Solubility} = \left[1 - \left(\frac{\textit{Dried sample weight} - \textit{dried filter weight}}{\textit{Sample weight}}\right)\right] * 100 \quad (1)$$

3. Results and discussion

3.1. Results: characterization

3.1.1. Physical characterization

Results of moisture, ashes, pH and density are presented in Table 1.

The first point to mention is that around half of the wet weight of the material is water. In fact, this aspect is key to identifying circular economy strategies for two reasons. The first is that this high moisture is responsible for the sticky characteristics of the material, making its transport and direct handling very difficult during subsequent reprocessing. The second one is that this moisture is mainly due to the retained magnesium nitrate solution, which can produce nitrate leachate. For this reason and according to the European Waste Catalogue, this residue can be classified as a "waste containing hazardous substances" within the group "wastes from the manufacture, formulation, supply and use of nitrogen chemicals, nitrogen chemical processes and fertilizer manufacture", with the code 06 10 02* (Eurostat, 2010). Therefore, the material has to be managed as a hazardous industrial sludge, with all the economic, legal and environmental implications that this entails.

Also noticeable was the low percentage of ashes obtained, 26 %, much lower than that expected for an inorganic material like this. The presence of a significant amount of organic matter was discounted due to the nature of the production process, so this high weight reduction during calcination must be due to the thermal decomposition of one or more of the components of the material. In this regard, it is well known that magnesium nitrate undergoes thermal decomposition to produce magnesium oxide, nitrogen dioxide and oxygen (Eq. 2) at temperatures above 300 °C (Prieto et al., 2019).

$$2Mg(NO_3)_2 \rightarrow 2MgO + 4NO_2 + O_2 \quad (2)$$

Table 1
Physical analyses of the muddy residue.

Parameter	Value
Moisture (%)	47 ± 4
Ashes (%)	26 ± 2
pH	7.3 ± 0.2
Density (g/ml)	0.85 ± 0.02

The significant mass loss at high temperatures is also a crucial factor in determining alternative ways of management for the material. This implies that the material is not suitable for use as a raw material for the refractory or cement industries or any sector in which high temperatures are required during the production process, due to the high emissions of nitric oxides.

The pH was close to neutrality, which suggests that the nitric acid was not dosed in excess.

3.1.2. Chemical characterization

Quantitative analysis by X-ray fluorescence (XRF) allows the identification of the chemical composition of the material, expressed as oxides (see Table 2).

The results reveal that magnesium and silicon are the main components of this material. The presence of the former is due to unreacted magnesite and/or crystallized magnesium nitrate, whereas silicon oxides are refractory to the nitric acid attack. Aluminium and iron were also detected as minor compounds, most probably in the form of oxides. Finally, calcium, titanium, phosphorus, potassium, manganese and sodium were detected as trace elements. It should be stressed that loss on ignition (LOI, 950 °C) corresponded to more than half of the total mass, which corroborates the high proportion of nitrate in the composition of the material. In order to determine the presence of those elements which were not detected due to their likely volatilization as LOI during the XRF analyses, an EDX analysis was also carried out. This technique revealed the presence of nitrogen (13 ± 1 %) and oxygen (68 ± 2 %) in the material, confirming the LOI and percentage of ashes previously obtained.

Therefore, it can be concluded that nitrogen, oxygen and magnesium are the main elements in the residue. It is worth mentioning that, with regard to proposing circular economy strategies, these results suggest that significant percentages of insolubilized nitrogen and magnesium still remain in the solid residue obtained during the production of aqueous magnesium nitrate fertilizer, which opens the door to its reuse in the same plant where it was generated. Nonetheless, this alternative requires pretreatment of the material to improve its mechanical properties and handling, as mentioned below. Iron, aluminium, calcium and silicon appear as minority components, none of them limiting the reuse of the material as fertilizer.

In order to obtain more information about the use of this material as a solid fertilizer, its cation exchange capacity (CEC) was measured. This parameter refers to the number of negative charges available on the surface of the material and gives an indication of its potential to hold plant nutrients, by estimating the capacity to retain cations. Soils with high CEC are typically considered to be more fertile, as they can hold more plant nutrients (McGrath et al., 2014). The CEC for the material under study was 31 ± 6 meq/100 g. This value indicated that the incorporation of this material into soils, as well as releasing nitrogen and magnesium as nutrients, also increases the CEC of poor soils such as those with a sandy loam or even clayey texture, all of them typically having CEC values lower than 30 (Lagouin et al., 2021; Meimaroglou and Mouzakis, 2019).

Table 2
Chemical composition and trace elements of the muddy residue determined by XRF.

Compound	Percentage (%)
MgO	16.2 ± 0.7
SiO_2	15.7 ± 0.9
Fe_2O_3	6.3 ± 0.3
Al_2O_3	3.1 ± 0.2
CaO	0.8 ± 0.3
P_2O_5	0.16 ± 0.02
TiO_2	0.15 ± 0.01
K_2O	0.12 ± 0.02
MnO	0.09 ± 0.01
Na_2O	0.05 ± 0.01
Loss on ignition (LOI)	57 ± 2

3.1.3. Structural characterization

Once the main elements of the material were identified, its structural characterization was carried out by means of XRD measurements. The diffraction patterns of the insoluble fraction obtained during the production of aqueous magnesium nitrate fertilizer by the attack of magnesite using nitric acid are depicted in Fig. 1.

The pattern showed the heterogeneous nature of this residue, consisting of a mixture of crystalline phases. In addition to magnesium nitrate (also known as nitromagnesite), as was previously proposed, the evaluation of the distinct diffraction lines showed the presence of yoderite ($Mg_2(Al,Fe)_6(SiO_4)O_2(OH)_2$), as the main insolubilized impurity in the initial magnesite (Callegari et al., 2021). In fact, yoderite formation is often associated with the magnesian metasomatism of an argillaceous sandstone, thus explaining its presence in the magnesite rock and its appearance in the final insoluble residue after the nitric acid attack (Johnson and Oliver, 2004). Other constituents include quartz (SiO_2) and silicates: ferrosilite ($FeSiO_3$), pyrophyllite ($Al_2Si_4O_{10}(OH)_2$) and hedenbergite ($CaFeSi_2O_6$).

The semi-quantification of the proportions (in mass fraction) of each of the identified crystalline phases was performed using the normalized RIR method (Chipera and Bish, 2013) and the values obtained are shown in Table S1 in the Supplementary Material. They show that 63.2 % of this residue is attributed to yoderite and nitromagnesite. These results are in accordance with those obtained by XRF, which indicated that magnesium and silicon are the main elements found in the residue.

These results were also consistent with those obtained by FTIR spectroscopy (Fig. 2), which provides valuable information about the structure and also decisive indications of the functional groups of the various compounds found in the residue.

The bands observed at 3200–3400 cm^{-1} and the peak at 1631 cm^{-1} are attributed to the stretching and bending modes of hydroxyl groups of the hydrated compounds observed in the muddy residue (Qiao et al., 2021). The strong band at 1382 cm^{-1}, medium band at 1076 cm^{-1} and medium peak at 825 cm^{-1} can be assigned to the asymmetric and symmetric stretching and out-of-plane bending modes of the nitrate ion of nitromagnesite (Bishop et al., 2021; Sulaiman et al., 2013). It should be noted that the region from 1100 to 800 cm^{-1} is also characteristic of the stretching mode of Si-O-Si found in silicates and quartz, and thus overlaps with the nitrate ion vibration modes (Ellerbrock et al., 2022). The weak absorption bands identified from 3000 to 1700 cm^{-1} may be due to the overtone and combination modes of the nitrate ion of nitromagnesite (Bishop et al., 2021). The band at 610 cm^{-1} can be attributed to the Si-O-Al bending vibration of pyrophyllite or yoderite and it overlaps with the Si-O-Si bending vibration commonly present in silicates (Bishop, 2018; Loganathan et al., 2013). Different components exhibited IR absorptions at around 468 cm^{-1}, including the Al—O bending vibration due to yoderite or pyrophyllite, the Fe—O bending vibrations associated with yoderite or ferrosilite and the Si-O-Si rocking vibration typically found in silicates (Jiang et al., 2023; Jozanikohan and Abarghooei, 2022).

3.2. Textural characterization

In order to evaluate its potential use as a cost-effective adsorbent, the surface area and the kind of porosity were first studied thoroughly. The specific surface area (BET area), pore volume and pore size were determined using nitrogen adsorption-desorption at 77 K. As can be seen in Fig. S2 in the Supplementary Material, the isotherm exhibits a characteristic hysteresis loop, which is associated with capillary condensation taking place in mesopores, and the limiting uptake over a range of high P/P_o. According to the IUPAC classification of adsorption isotherms, this pattern is typical of type IV(a) isotherms (Thommes et al., 2015). The initial part of the isotherm is attributed to monolayer-multilayer adsorption. It forms when lateral interactions between adsorbed molecules are weak in comparison to interactions between the adsorbent surface and adsorbate. Such isotherms

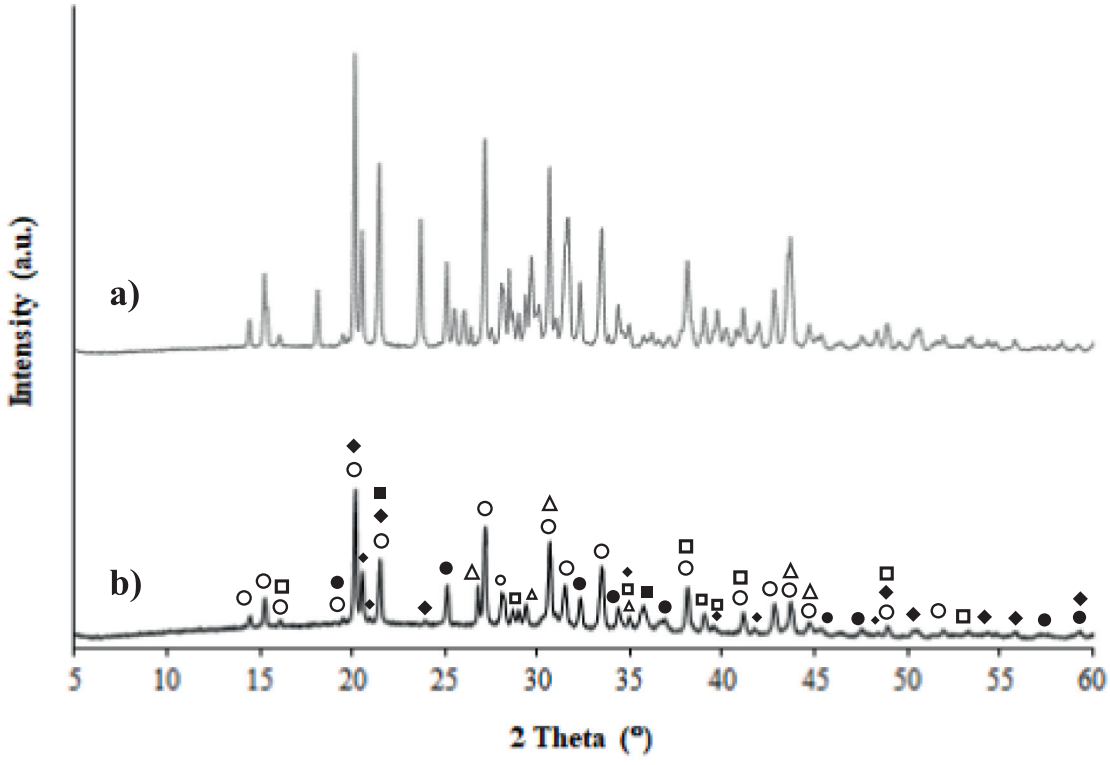

Fig. 1. XRD pattern of the pure nitromagnesite (a) and the muddy residue (b). Identified phases: nitromagnesite (○), yoderite (●), quartz (■), ferrosilite (Δ), pyrophyllite (♦) and hedenbergite (□).

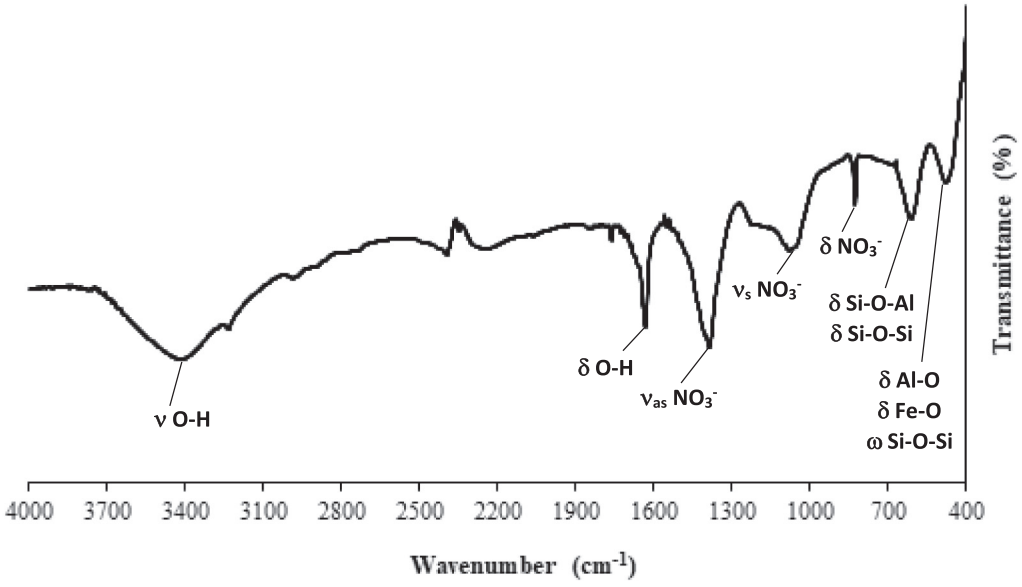

Fig. 2. FTIR of the muddy residue from 400 to 4000 cm^{-1}.

are characteristic of many mesoporous industrial adsorbents. The isotherm also exhibited a narrow hysteresis loop, which can be classified as type H3 and is linked to the filling and emptying of mesopores by capillary condensation and evaporation, respectively. This type of hysteresis loop is characterized by the presence of slit-shaped pores (Yurdakal et al., 2019). The low nitrogen adsorption at a value of P/P_o lower than 0.2 suggests the absence of significant microporosity in the material. In addition, at P/P_o around 1, the adsorption limit is not clearly defined, revealing the existence of macroporosity.

Specific surface areas were determined using the Brunauer-Emmett-Teller (BET) method. The adsorption and desorption branches of the N_2 isotherms allowed us to obtain the mesoporosity characteristics. Thus, the material exhibited a specific surface area of 20 ± 3 m^2/g and a pore volume of 0.14 ± 0.02 cm^3/g, with an average pore diameter of 22.5 ± 0.5 nm.

3.2.1. Morphological characterization

In order to corroborate the previously mentioned findings, SEM and TEM microscopy analyses were carried out (Fig. 3).

The SEM micrographs shown in Fig. 3a and b sustain the existence of a heterogeneous mixture of particle aggregates with different sizes and shapes. Among these shapes, the morphological analysis shows the predominance of leaf layout, with eroded and rounded particles and a laminated structure, which is typical of phyllosilicates. The phyllosilicates, or sheet silicates, are an important group of minerals, including yoderite and pyrophyllite. Besides, they are one of the most abundant constituents of

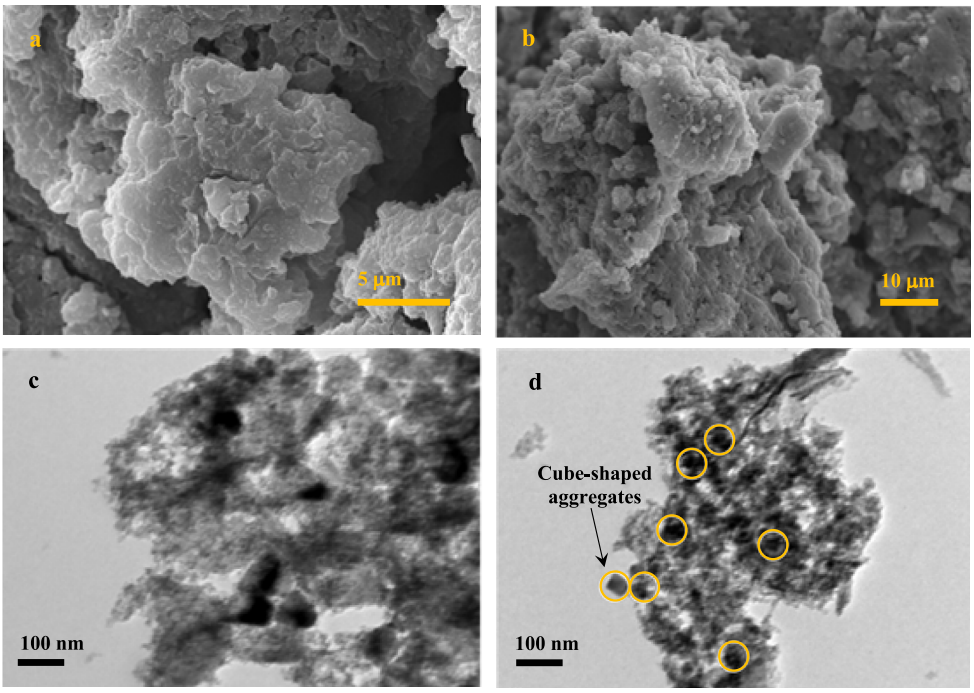

Fig. 3. SEM images for the muddy residue at a magnification of: ×5000 (a) and ×1500 (b). TEM images of the muddy residue at a magnification of ×100,000 (c, d).

sedimentary rocks, as is the magnesite mineral employed as raw material (Boggs, 2009).

Apart from this, Fig. 3a shows the interparticular cavities likely to be responsible for the macroporous structure of the muddy residue observed during the BET analyses.

By means of a TEM analysis, the laminar structure was corroborated, as can be seen in Fig. 3c and d. As the sample is not compactly aggregated, TEM images also allowed a better examination of the pore structure of the material. Slit-like pores were observed, this geometry being characteristic of the H3 type hysteresis, which is in accordance with the textural characterization mentioned in the previous section (Andrunik et al., 2023; Foster et al., 2014). Finally, Fig. 3d shows the presence of cube-shaped aggregates in the residue, with an average particle size of 25 nm.

Finally, the material was also subjected to HAABF-STEM analyses, which provide higher resolution images at the atomic scale, as well as making it possible to distinguish the distribution of the main components on the surface of the material (Fig. 4).

It is interesting to point out that the elemental mapping showed that the presence of nitrogen in the residue is much lower than that expected from the significant mass loss at high temperatures previously reported. In this sense, it is important to emphasize that this element could be affected by local overheating of the residue caused by the electron beam which would hinder its detection. The mapping does show great abundance of oxygen, which is consistent with the high percentage of oxides in the samples (see Table 2). Taking into account the similar dispersions observed in Fig. 4c, d and f, it is reasonable to deduce that these oxides are mainly silicates (which were not solubilized by the nitric acid) and different compounds of magnesium such as nitromagnesite (precipitate obtained after nitric acid attack of magnesite) and yoderite (silicate with magnesium in its composition). The low densities observed during the mapping of calcium (Fig. 4 h) agree with the small proportion of hedenbergite in the material, whereas the presence of carbon (Fig. 4e) may be due to the surface carbonation of the unreacted nitromagnesite during its storage.

3.3. Discussion: reuse options

As previously explained, the high proportion of nitrates in the residue obtained from magnesium nitrate production limits its use in manufacturing processes where the raw materials have to be exposed to high temperatures. So, options such as the reuse of this residue in cement, ceramic, glass or refractory fabrication must be discarded. However, considering its composition (rich in nitrogen, magnesium and calcium, among other compounds) and its physicochemical properties (neutral pH, low density, high CEC), the most feasible alternative for reusing the residue obtained from the magnesium nitrate production may well be its reintroduction in the fertilizer manufacturing process. This strategy means that the residue obtained from the magnesium nitrate production can be managed within the production plant itself, which complies with another principle of circular economy, the proximity between the stakeholders in the procurement process (Witjes and Lozano, 2016).

In this light, two different approaches were proposed for reusing this residue in the fertilizer industry depending on its state of aggregation: solid or liquid. At this point, although these approaches will be discussed in more depth below, it is interesting to note that they are complementary and not mutually exclusive.

3.3.1. Reuse for production of solid fertilizers

The mud-like characteristic of the residue obtained from magnesium nitrate production is probably one of the main limitations associated with its potential use as a raw material for the production of solid fertilizers. The viscous, sticky properties of this material make its industrial handling very difficult, generating obstructions and problems associated with mixing, pumping and milling, among others. This is the reason why a mechanical characterization of the sample was also carried out.

With this aim, firmness and stickiness were determined. It was found that this residue from magnesium nitrate production had a firmness value of 270 ± 10 g and a stickiness of 120 ± 10 g, corroborating the very poor flow properties. Therefore, previous treatment is imperative in order to improve its handling before being incorporated into the solid fertilizer production line.

Different hardening agents were tested for this purpose. These agents, which included beach sand, dolomite, magnesite, gypsum, quicklime and Portland cement, were chosen on the basis of their low cost and availability in conventional fertilizer production plants. The firmness and stickiness values determined after the addition of 5 % or 15 % of the corresponding hardening agent are shown in Fig. S3 in the Supplementary Material.

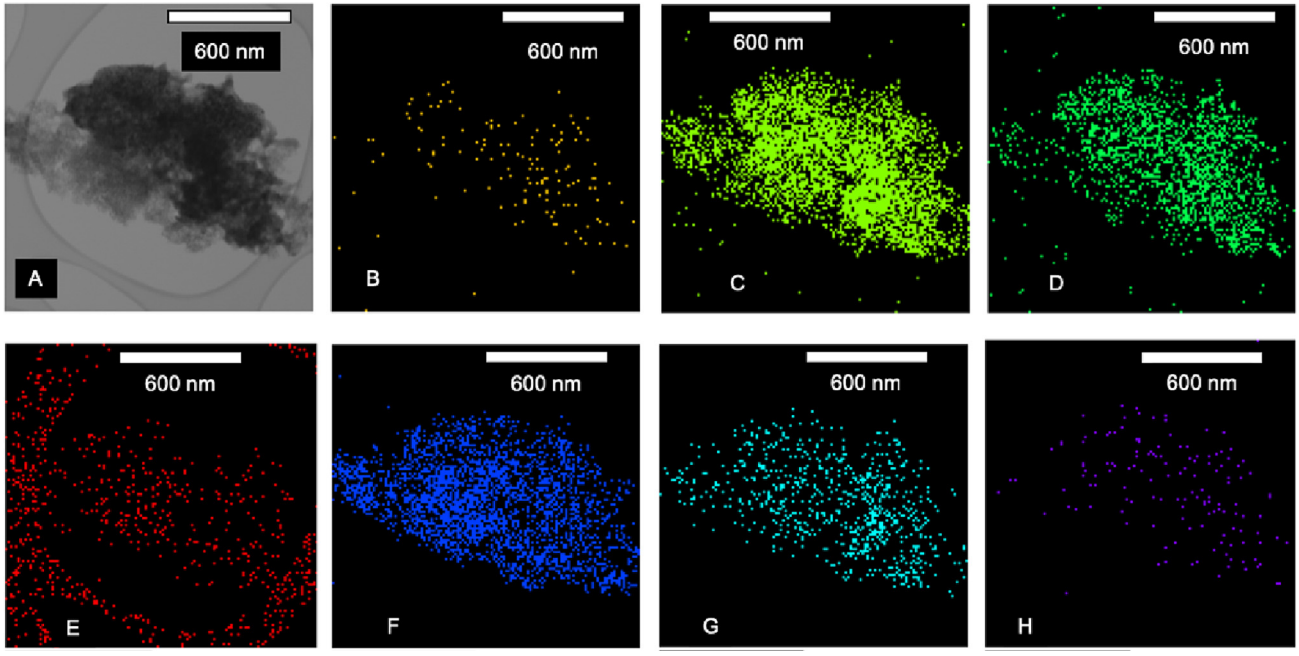

Fig. 4. STEM image of the muddy residue (A) and the corresponding elemental mapping: Nitrogen (B), Oxygen (C), Magnesium (D), Carbon (E), Silicon (F), Aluminium (G) and Calcium (H).

Hardening agents were not added at percentages higher than 15 % in order not to cause a disproportionate consumption of these or an excessive dilution of nitrogen and magnesium in the final mixture.

It was found that all the potential hardening agents tested had a negative effect on the firmness of the final mixture, which implies lower hardness and, hence, a deterioration in its handling. Nevertheless, these agents did reduce the stickiness of the sample, thus reducing blockage problems in the pipeline during processing. Despite this, as visual and tactual checks also showed, none of these agents provided a sufficient improvement in the mechanical properties to incorporate them directly into the production line.

The moisture levels of the final mixtures corresponding to each hardening agent were experimentally measured and compared with the theoretical ones, obtained from a water mass balance carried out for the residue from the magnesium nitrate production and the hardening agent. Only when sand, cement or quicklime were added, was the experimental moisture lower than the theoretical value (see Table S2 in the Supplementary Material). Hence, it can be concluded that these agents are desiccants, acting as water sequestrants by sorption (sand) or by reaction (Portland cement and quicklime, Eqs. 3, 4 and 5) (Kurdowski, 2014).

$$2Ca_3SiO_5 + 7H_2O \rightarrow 3CaO.2SiO_2.4H_20 + 3Ca(OH)_2 \quad (3)$$

$$2Ca_2SiO_4 + 5H_2O \rightarrow 3CaO.2SiO_2.4H_20 + Ca(OH)_2 \quad (4)$$

$$CaO + H_2O \rightarrow Ca(OH)_2 \quad (5)$$

Therefore, desiccants caused the lowest moisture and also, the highest firmness values, which suggests that these two parameters are interlinked with each other. According to experiments, Portland cement and, especially, quicklime seem to be the most adequate options to improve the mechanical properties of the residue obtained from magnesium nitrate production. A more detailed picture of the changes in firmness and stickiness values, testing different percentages of cement or quicklime (from 0 to 30 %), is shown in Fig. 5.

It is easily deduced that both quicklime and Portland cement cause the firmness of the residue to rise, reaching relatively high hardness after the mixing process, and allowing its processing in the conventional solid fertilizer plant. Nevertheless, the two agents differed in the way the stickiness changed when the dosage was increased. The stickiness values reached a minimum for 7 % cement and then gradually increased for higher cement dosages, thus generating a harder but also stickier final material. On the other hand, when quicklime was employed, stickiness values also increased, but a maximum was reached for a dosage of 10 % and then they fell rapidly, even achieving stickiness values lower than the initial one at quicklime dosages higher than 25 %. In conclusion, a hard, but easily disaggregated, non-sticky material is obtained by using quicklime, in such a way that it could be correctly processed within the fertilizer plant and incorporated with the solid fertilizer.

The use of quicklime as the "conditioner", as well as improving the handling, also adds calcium to the final solid fertilizer. Calcium is widely recognized for its ability to help maintain a chemical balance in the soil, reducing soil salinity, and improving water penetration when it is used as the soil amendment. It plays an important function in plants by increasing nutrient uptake, building strong cell walls for sturdier plants, and increasing vitality (Behnood, 2018; Rhodes et al., 2018). It can easily be deduced by mass balances that, with a 30 % dosage of quicklime, the resulting material contains 5.7 %, 5.0 % and 24.3 % in dry weight of magnesium, nitrogen and calcium, respectively. Therefore, its incorporation into a solid fertilizer does not entail the impoverishment of the nutrient composition of the final product.

3.3.2. Reuse for production of liquid fertilizers

Parallel to the utilization of the residue obtained from magnesium nitrate production in solid fertilizer, the high percentage of nitromagnesite remaining in this waste material can be solubilized to produce liquid fertilizers. By this means, solutions with a variable composition of magnesium nitrate are obtained, while, at the same time, the mass of residue is reduced.

In order to assess the viability of this alternative, the solubilities of the residue in water and nitric acid (37 %) were tested. These solvents were chosen because of their low cost and availability in a conventional fertilizer plant.

Fig. 6 shows the remaining mass of residue at the end of solubilization experiments with water or nitric acid, as well as the amount of insolubilized magnesium nitrate, determined by XRD.

As can be seen, carrying out a subsequent washing of the residue with either water or nitric acid has two positive effects on the handling of this material: a reduction in the final mass of dry solid to be managed and a significant decrease in the amount of magnesium and nitrogen wasted during the conventional disposal of the residue. Regarding the former, reductions in the dry mass of 70 % and 77 % were achieved with water and nitric acid, respectively. The higher solubilization obtained with nitric acid than with water was expected, since the initial acidic attack on the calcined magnesite mineral was also carried out with nitric acid, this being much more aggressive than water. However, it should be taken into account that the loss of a small percentage of the material as fine solids is likely. Regarding the recovery of magnesium and nitrogen from the solid residue, only 19 % and 14 % of the initial nitromagnesite were not solubilized by water and nitric acid, respectively, resulting in liquid fertilizers with around 16 % magnesium nitrate in their composition, far from negligible percentage considering that the concentration of magnesium nitrate in conventional liquid fertilizers is usually 35 %. Therefore, these findings indicate another way of reusing the residue obtained from magnesium nitrate production within the same plant, by washing this waste with water or, better, with nitric acid. The magnesium nitrate solution obtained could be then enriched to the 35 % concentration demanded by consumers by a subsequent acidic attack on the raw rock.

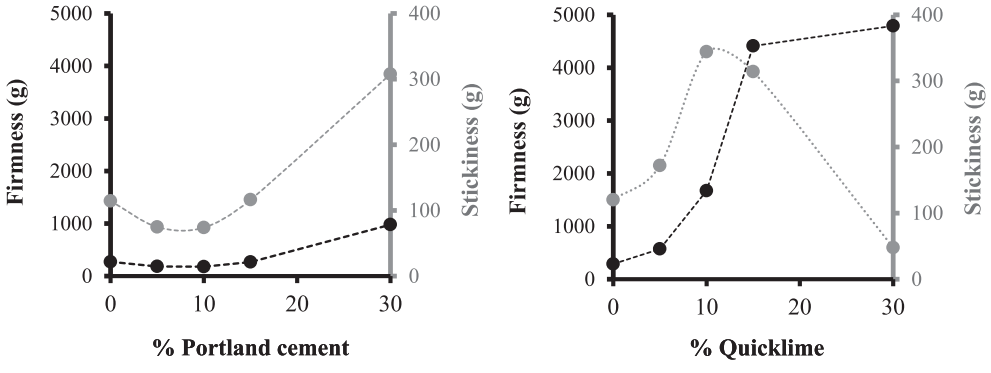

Fig. 5. Firmness and stickiness values of the muddy residue after adding different percentages of quicklime (a) or Portland cement (b).

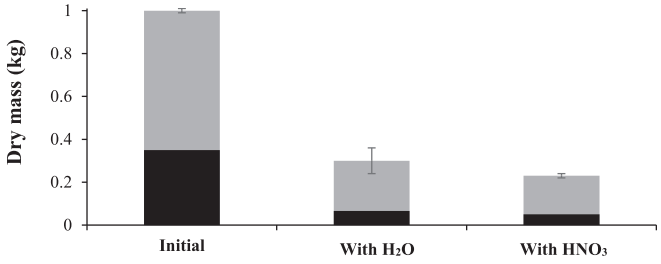

Fig. 6. Insolubilized total (■) and magnesium nitrate (■) masses after the solubility tests of the muddy residue with water or nitric acid (37 %).

4. Conclusions

The characterization of the residue obtained from magnesium nitrate production revealed that it is a soft sticky material, with 47 % moisture content, a neutral pH and a specific density of 0.85. It is mainly composed of nitromagnesite (formed during the reaction of nitric acid with magnesium oxide in the production of the fertilizer), and this corresponds to 35 % of the dry weight, which leads to high mass losses on ignition (LOI). Other constituents include quartz and different silicates of iron, aluminium and calcium. Structurally, the material is predominantly mesoporous, with slit-like pores, a specific surface area of 20 ± 3 m^2/g and a cation exchange capacity of 31 ± 6 meq/100 g.

Based on these properties and on the principles of circular economy, the most feasible alternative for reusing this residue obtained from magnesium nitrate production was found to be its reintroduction in the manufacturing process of solid or liquid fertilizers. For the former, the residue obtained from magnesium nitrate production has to be mixed with 30 % quicklime in order to improve its mechanical properties, resulting in a material that contains 5.7 %, 5.0 % and 24.3 % dry weight of magnesium, nitrogen and calcium, respectively. In parallel, around 86 % of the remaining nitromagnesite in the residue can be recovered by rewashing it with nitric acid, obtaining a liquid fertilizer with 16 % magnesium nitrate and, simultaneously, reducing the initial dry mass of the residue by 77 %.

CRediT authorship contribution statement

Sergio Collado: Conceptualization, Methodology, Writing – review & editing, Visualization. **Paula Oulego:** Conceptualization, Formal analysis. **Silvia Vázquez:** Investigation, Data curation, Writing – original draft, Visualization. **Lucía Pola:** Writing – review & editing. **Mario Díaz:** Funding acquisition, Project administration, Supervision, Writing – review & editing.

Data availability

Data will be made available on request.

Declaration of competing interest

The authors declare that they have no known competing financial interests or personal relationships that could have appeared to influence the work reported in this paper.

Acknowledgements

The authors wish to express their deepest gratitude to Fertiberia Avilés (Spain), who generously provided us with the material and information about the production process of liquid fertilizers. The authors are also grateful for financial support from the Employment, Industry and Tourism Office of the Principality of Asturias (Spain) through the project SV-PA-21-AYUD/2021/51041 and for that received from the State Research Agency (Spanish Ministry of Science, Innovation and Universities) through the projects MCIU-19-RTI2018-094218-B-I00 and MCIU-22-PID2021-125942OB-I00.

Appendix A. Supplementary data

Supplementary data to this article can be found online at https://doi.org/10.1016/j.scitotenv.2023.162925.

References

Abdel-Aal, E., Rashad, M., 1997. Hydrometallurgical processing of egyptian magnesite ore with nitric acid. Physicochem. Probl. Mi 31, 7–17.
Alemrajabi, M., Rasmuson, Å.C., Korkmaz, K., Forsberg, K., 2019. Processing of a rare earth phosphate concentrate obtained in the nitrophosphate process of fertilizer production. Hydrometallurgy 189, 105144. https://doi.org/10.1016/j.hydromet.2019.105144.
Alshameri, A., He, H., Zhu, J., Xi, Y., Zhu, R., Ma, L., Tao, Q., 2018. Adsorption of ammonium by different natural clay minerals: characterization, kinetics and adsorption isotherms. Appl. Clay Sci. 159, 83–93. https://doi.org/10.1016/j.clay.2017.11.007.
Andrunik, M., Skalny, M., Bajda, T., 2023. Functionalized adsorbents resulting from the transformation of fly ash: characterization, modification, and adsorption of pesticides. Sep. Purif. Technol. 309, 123106. https://doi.org/10.1016/j.seppur.2023.123106.
Baltrusaitis, J., Sviklas, A.M., 2016. From insoluble minerals to liquid fertilizers: magnesite as a source of magnesium (Mg) nutrient. ACS Sustain. Chem. Eng. 4, 5404–5408. https://doi.org/10.1021/acssuschemeng.6b01621.
Behnood, A., 2018. Soil and clay stabilization with calcium- and non-calcium-based additives: a state-of-the-art review of challenges, approaches and techniques. Transp. Geotech. 17, 14–32. https://doi.org/10.1016/j.trgeo.2018.08.002.
Bishop, J.L., 2018. Chapter 3 - remote detection of phyllosilicates on Mars and implications for climate and habitability. In: Cabrol, N.A., Grin, E.A. (Eds.), From Habitability to Life on Mars. Elsevier, pp. 37–75.
Bishop, J.L., King, S.J., Lane, M.D., Brown, A.J., Lafuente, B., Hiroi, T., Roberts, R., Swayze, G.A., Lin, J.-F., Sánchez, M., 2021. Spectral properties of anhydrous carbonates and nitrates. Earth Space Sci. 8, e2021EA001844. https://doi.org/10.1029/2021EA001844.
Boggs Jr., S., 2009. Petrology of Sedimentary Rocks. 2nd ed. Cambridge University Press, Cambridge https://doi.org/10.1017/CBO9780511626487.
Callegari, A.M., Boiocchi, M., Day, M.C., Hawthorne, F.C., 2021. Crystal structure, EMPA and FTIR spectroscopy of green yoderite, (Mg2.02Al5.68Fe3 + 0.35)Σ8.05(Si3.93 P5 + 0.03)Σ3.96O18(OH)2, from Mautia HillTanzania. Period. Mineral. 90, 371–381. https://doi.org/10.13133/2239-1002/17556.
Chipera, S.J., Bish, D.L., 2013. Fitting full X-ray diffraction patterns for quantitative analysis: a method for readily quantifying crystalline and disordered phases. Adv. Mater. Phys. Chem. 3, 47–53. https://doi.org/10.4236/ampc.2013.31A007.
Chojnacka, K., Moustakas, K., Witek-Krowiak, A., 2019. Bio-based fertilizers: a practical approach towards circular economy. Bioresour. Technol. 122223. https://doi.org/10.1016/j.biortech.2019.122223.
Intelligence, M., 2019. Europe liquid fertilizer market - growth, trends, and forecast (2019 - 2024). In: Intelligence, M. (Ed.), Industry Reports, India, p. 109.
Ellerbrock, R., Stein, M., Schaller, J., 2022. Comparing amorphous silica, short-range-ordered silicates and silicic acid species by FTIR. Sci. Rep. 12, 11708. https://doi.org/10.1038/s41598-022-15882-4.
Eurostat, 2010. Guidance on classification of waste according to EWC-Stat categories. . https://ec.europa.eu/eurostat/documents/342366/351806/Guidance-on-EWCStat-categories-2010.pdf. (Accessed 3 February 2023).
Eurostat, 2022. Consumption of Inorganic Fertilizers. accessed 23 June 2022 http://appsso.eurostat.ec.europa.eu/nui/show.do?dataset=aei_fm_usefert&lang=en.
FAO, 2019. World Fertilizer Trends and Outlook to 2022. Rome.
Foster, J.A., Johnson, D.W., Pipenbrock, M.-O.M., Steed, J.W., 2014. Using gel morphology to control pore shape. New J. Chem. 38, 927–932. https://doi.org/10.1039/C3NJ01295F.
García-Saldaña, A., Landeros-Sánchez, C., Castañeda-Chávez, M., Martínez-Dávila, J.P., Pérez-Vázquez, A., Carrillo-Ávila, E., 2019. Fertirrigation with low-pressure multi-gate irrigation systems in sugarcane agroecosystems: a review. Pedosphere 29, 1–11. https://doi.org/10.1016/S1002-0160(18)60053-0.
Gee, E.A., Pawel, M.T., 1951. Production of magnesium chloride from magnesium silicate ore US Pat No 2549798A.
Gugava, E., Korokhashvili, A., 2018. Technologies for obtaining nitrogen fertilizers prolonged effect in wheat. Ann. Agrar. Sci. 16, 22–26. https://doi.org/10.1016/j.aasci.2017.12.003.
Guo, W., Nazim, H., Liang, Z., Yang, D., 2016. Magnesium deficiency in plants: an urgent problem. Crop J. 4, 83–91. https://doi.org/10.1016/j.cj.2015.11.003.
Jiang, C., Ramteke, D.D., Li, J., Sliz, R., Sreenivasan, H., Cheeseman, C., Kinnunen, P., 2023. Preparation and characterization of binary mg-silicate glasses via sol-gel route. J. Non-Cryst. Solids 606, 122204. https://doi.org/10.1016/j.jnoncrysol.2023.122204.
Johnson, S.P., Oliver, G.J.H., 2004. A second natural occurrence of yoderite. J. Metamorph. Geol. 16 (6), 809–818. https://doi.org/10.1111/j.1525-1314.1998.00172.x.
Jozanikohan, G., Abarghooei, M.N., 2022. The Fourier transform infrared spectroscopy (FTIR) analysis for the clay mineralogy studies in a clastic reservoir. J. Pet. Explor. Prod. Technol. 12, 2093–2106. https://doi.org/10.1007/s13202-021-01449-y.
Kurdowski, W., 2014. Cement and concrete chemistry. Springer Science & Business, New York.
Lagouin, M., Aubert, J.-E., Laborel-Préneron, A., Magniont, C., 2021. Influence of chemical, mineralogical and geotechnical characteristics of soil on earthen plaster properties. Constr. Build. Mater. 304, 124339. https://doi.org/10.1016/j.conbuildmat.2021.124339.
Li, Y., Xu, J., Liu, X., Liu, B., Liu, W., Jiao, X., Zhou, J., 2022. Win-win for monosodium glutamate industry and paddy agriculture: replacing chemical nitrogen with liquid organic fertilizer from wastewater mitigates reactive nitrogen losses while sustaining yields. J. Clean. Prod. 347, 131287. https://doi.org/10.1016/j.jclepro.2022.131287.

Lipps, W.C., Braun-Howland, E.B., Baxter, T.E., 2023. Standard methods for the examination of water and wastewater. APHA-AWWA-WEF, 24th ed. APHA Press, Washington, D.C.

Loganathan, S., Tikmani, M., Ghoshal, A.K., 2013. Novel pore-expanded MCM-41 for CO2 capture: synthesis and characterization. Langmuir 29 (10), 3491–3499. https://doi.org/10.1021/la400109j.

Matamoros, V., Casas, M.E., Mansilla, S., Tadić, Đ., Cañameras, N., Carazo, N., Portugal, J., Piña, B., Bayona, J.M., 2022. Occurrence of antibiotics in Lettuce (Lactuca sativa L.) and radish (Raphanus sativus L.) following organic soil fertilisation under plot-scale conditions: crop and human health implications. J. Hazard. Mater. 436, 129044. https://doi.org/10.1016/j.jhazmat.2022.129044.

Matta, S., Stephan, K., Stephan, J., Lteif, R., Goutaudier, C., Saab, J., 2017. Phosphoric acid production by attacking phosphate rock with recycled hexafluosilicic acid. Int. J. Miner. Process. 161, 21–27. https://doi.org/10.1016/j.minpro.2017.02.008.

McGrath, J.M., Spargo, J., Penn, C.J., 2014. Soil fertility and plant nutrition. Encyclopedia of Agriculture and Food Systems. 166–184. https://doi.org/10.1016/b978-0-444-52512-3.00249-7.

Meimaroglou, N., Mouzakis, C., 2019. Cation exchange capacity (CEC), texture, consistency and organic matter in soil assessment for earth construction: the case of earth mortars. Constr. Build. Mater. 221, 27–39. https://doi.org/10.1016/j.conbuildmat.2019.06.036.

Oulego, P., Laca, A., Calvo, S., Díaz, M., 2020. Eggshell-supported catalysts for the advanced oxidation treatment of humic acid polluted wastewaters. Water 12, 100. https://doi.org/10.3390/w12010100.

Pressi, G., Barbieri, E., Rizzi, R., Tafuro, G., Costantini, A., Domenico, E.D., Semenzato, A., 2022. Formulation and physical characterization of a polysaccharidic gel for the vehiculation of an insoluble phytoextract for mucosal application. Polysaccharides 3 (4), 728–744. https://doi.org/10.3390/polysaccharides3040042.

Prieto, C., Ruiz-Cabañas, F.J., Rodríguez-Sanchez, A., Rubio, C., Fernández, A.I., Martínez, M., Oró, E., Cabeza, L.F., 2019. Effect of the impurity magnesium nitrate in the thermal decomposition of the solar salt. Sol. Energy 192, 186–192. https://doi.org/10.1016/j.solener.2018.08.046.

Qiao, Y., Theyssen, N., Spliethoff, B., Folke, J., Weidenthaler, C., Schmidt, W., Prieto, G., Ochoa-Hernández, C., Bill, E., Ye, S., Ruland, H., Schüth, F., Leitner, W., 2021. Synthetic ferripyrophyllite: preparation, characterization and catalytic application. Dalton Trans. 50, 850–857. https://doi.org/10.1039/d0dt03125a.

Rhodes, R., Miles, N., Hughes, J.C., 2018. Interactions between potassium, calcium and magnesium in sugarcane grown on two contrasting soils in South Africa. Crops Res. 223, 1–11. https://doi.org/10.1016/j.fcr.2018.01.001.

Saadaoui, E., Ghazel, N., Romdhane, C.B., Massoudi, N., 2017. Phosphogypsum: potential uses and problems – a review. Int. J. Environ. Stud. 74 (4), 558–576. https://doi.org/10.1080/00207233.2017.1330582.

Saejiew, A., Grunberger, O., Arunin, S., Favre, F., Tessier, D., Boivin, P., 2004. Critical coagulation concentration of paddy soil clays in sodium-ferrous iron electrolyte. Soil Sci. Soc. Am. J. 68, 789–794.

Singh, R., Singh, H., Raghubanshi, A.S., 2019. Challenges and opportunities for agricultural sustainability in changing climate scenarios: a perspective on indian agriculture. Trop. Ecol. 60, 167–185. https://doi.org/10.1007/s42965-019-00029-w.

Smol, M., 2021. Transition to circular economy in the fertilizer sector – analysis of recommended directions and end-users' perception of waste-based products in Poland. Energies 14, 4312. https://doi.org/10.3390/en14144312.

Sulaiman, M., Rahman, A., Mohamed, N., 2013. Structural, thermal and conductivity studies of magnesium nitrate–alumina composite solid electrolytes prepared via sol-gel method. Int. J. Electrochem. Sci. 8, 6647–6655.

Thommes, M., Kaneko, K., Neimark, A.V., Olivier, J.P., Rodriguez-Reinoso, F., Rouquerol, J., Sing, K.S.W., 2015. Physisorption of gases, with special reference to the evaluation of surface area and pore size distribution (IUPAC technical Report). Pure Appl. Chem. 87 (9–10), 1051–1069. https://doi.org/10.1515/pac-2014-1117.

Velenturf, A.P.M., Purnell, P., 2021. Principles for a sustainable circular economy. Sustain. Prod. Consum. 27, 1437–1457. https://doi.org/10.1016/j.spc.2021.02.018.

Wang, Z., Hassan, M.U., Nadeem, F., Wu, L., Zhang, F., Li, X., 2020. Magnesium fertilization improves crop yield in most production systems: a meta-analysis. Front. Plant Sci. 10, 1727. https://doi.org/10.3389/fpls.2019.01727.

Wang, H., Wu, L., Wang, X., Zhang, S., Cheng, M., Feng, H., Fan, J., Zhang, F., Xiang, Y., 2021. Optimization of water and fertilizer management improves yield, water, nitrogen, phosphorus and potassium uptake and use efficiency of cotton under drip fertigation. Agric. Water Manag. 245, 106662. https://doi.org/10.1016/j.agwat.2020.106662.

William, J.K., Neville, P.B., 1983. In: Office, E.P. (Ed.), Productionof Magnesium Nitrate Solutions. Stamicarbon BV, Germany, p. 9 Ep 0107870 B1 19870916 (EN).

Witjes, S., Lozano, R., 2016. Towards a more circular economy: proposing a framework linking sustainable public procurement and sustainable business models. Resour. Conserv. Recycl. 112, 37–44. https://doi.org/10.1016/j.resconrec.2016.04.015.

Wu, S., Wang, L., Zhao, L., Zhang, P., El-Shall, H., Moudgil, B., Huang, X., Zhang, L., 2018. Recovery of rare earth elements from phosphate rock by hydrometallurgical processes – a critical review. Chem. Eng. J. 335, 774–800. https://doi.org/10.1016/j.cej.2017.10.143.

Xie, C., Zhang, T., Wang, X., Zhong, B., Tang, S., 2018. Solid-liquid phase equilibria in aqueous solutions of four common fertilizers at 303.2 K and atmospheric pressure. Fluid Phase Equilib. 474, 131–140. https://doi.org/10.1016/j.fluid.2018.07.016.

Yousaf, M., Bashir, S., Raza, H., Shah, A.N., Iqbal, J., Arif, M., Bukhari, M.A., Muhammad, S., Hashim, S., Alkahtani, J., Alwahibi, M.S., Hu, C., 2021. Role of nitrogen and magnesium for growth, yield and nutritional quality of radish. Saudi J. Biol. Sci. 28, 3021–3030. https://doi.org/10.1016/j.sjbs.2021.02.043.

Yurdakal, S., Garlisi, C., Özcan, L., Bellardita, M., Palmisano, G., Marcì, G., Palmisano, L., 2019. Chapter 4 – (photo)catalyst characterization techniques: adsorption isotherms and BET, SEM, FTIR, UV-Vis, photoluminiscence, and electrochemical characterizations. Heterogeneous Photocatalysis. Elsevier, pp. 87–152 https://doi.org/10.1016/B978-0-444-64015-4.00004-3.